Journal of Alloys and Compounds 519 (2012) 92–96

Contents lists available at SciVerse ScienceDirect

Journal of Alloys and Compounds

journal homepage: www.elsevier.com/locate/jallcom

Magnetization reversal in the Cr-doped manganite $Bi_{0.3}Ca_{0.7}Mn_{0.75}Cr_{0.25}O_3$

R.R. Zhang[a,*], G.L. Kuang[a], L.H. Yin[b], Y.P. Sun[a,b]

[a] High Magnetic Field Laboratory, Chinese Academy of Sciences, Hefei 230031, People's Republic of China
[b] Key Laboratory of Materials Physics, Institute of Solid State Physics, Chinese Academy of Sciences, Hefei 230031, People's Republic of China

ARTICLE INFO

Article history:
Received 31 May 2011
Received in revised form
16 December 2011
Accepted 19 December 2011
Available online 8 January 2012

PACS:
75.60.JK
71.27.+a
71.30.+h
75.47.Lx

Keywords:
Magnetization reversal
Magnetic transition
Manganites

ABSTRACT

Detailed magnetic properties of polycrystalline $Bi_{0.3}Ca_{0.7}Mn_{0.75}Cr_{0.25}O_3$ are investigated. It is observed that this compound exhibits negative magnetization below the compensation temperature (T_{comp}) when magnetization–temperature (M–T) curves are measured in a field-cooled mode with low applied fields (H < 1030 Oe). Furthermore, the compound shows a canted-antiferromagnetic transition at 120 K and a peak with positive sign at 98 K. Below 98 K, M decreases with decreasing temperature, passes through a zero value (M = 0) around T_{comp} = 78.5 K, and continues to decrease steeply until 5 K. The maximum absolute value of M below T_{comp} was about 15 times as large as that above T_{comp}. Considering the fact that the observed behavior is similar to that in $GdCrO_3$, the phenomenon of the magnetization reversal in the Cr-doped manganite $Bi_{0.3}Ca_{0.7}Mn_{0.75}Cr_{0.25}O_3$ is suggested to originate from the antiparallel coupling of the Cr^{3+} moments and the canted $Mn^{3+/4+}$ moments.

1. Introduction

Mn-site substitution in charge ordered (CO) manganites have been shown to be a very powerful tool to gradually control the collapse of the CO regions into either ferromagnetic (FM) metallic or weakly FM insulting (FMI) regions [1–4]. Since Cr^{3+} has a $t_{2g}^3 e_g^0$ configuration which is identical to that of Mn^{4+}, the Cr doping manganites have been extensively studied in previous literatures [2,5–7]. $Bi_{1-x}Ca_xMnO_3$ is an interesting but less-studied CO system. Early works reveal that the CO temperature T_{CO} is much higher than that in the $La_{1-x}Ca_xMnO_3$ [8]. It is believed that the $6s^2$ lone pair of Bi^{3+} ions which orients toward a surrounding anion O^{2-} can produce a local distortion or even an hybridization between Bi:$6s^2$ orbitals and O:2p orbitals. This effect will reduce the mobility of e_g electron, thus favor CO [9,10]. Modulation of the CO by substituting Cr, Fe, V, and Ni in $Bi_{1-x}Ca_xMnO_3$ has been reported [11–14]. In this work, the phenomenon of the magnetization reversal (MR) is reported in the Cr-doped manganite $Bi_{0.3}Ca_{0.7}Mn_{0.75}Cr_{0.25}O_3$. The subject of magnetization reversal in oxides has received considerable attention in recent years, which is usually achieved by applying a large enough magnetic field in a direction opposite to the aligned moments. This property forms the basis of most magnetic recording and storage devices. But the phenomenon of the MR in response to a change in temperature (in a small magnetic field) is seldom observed. This effect occurs in some ferrimagnetic materials, which contain two or more different types of magnetic ions, or one magnetic ion occupies at different crystallographic sites, the magnetization is partially cancelled due to the antiferromagnetic (AFM) coupling of the magnetic sublattices with unequal values of magnetization. If the temperature dependence of the magnetization of the antiferromagnetically coupled sublattices is different, a MR can be observed sometimes.

Luan et al. studied the different evolution of CO with Cr content between Bi-rich and Bi-poor samples, and they found that 20% Cr doped Bi-poor sample $Bi_{0.24}Ca_{0.76}MnO_3$ showed a large negative magnetization value at low temperature [15], but they did not focus on it. Since no detailed magnetization studies exist for Cr doped Bi-poor compounds, we have performed detailed magnetization measurements on $Bi_{0.3}Ca_{0.7}Mn_{0.75}Cr_{0.25}O_3$. The results show clear evidence for a MR, resulting in a negative magnetization for low fields (≤1010 Oe) at low temperature in the process of field-cooling (FC) measurements. Moreover, the compensation temperature, corresponding to the temperature at which magnetization value is zero, strongly depends on the magnitude of the applied field. The results are analyzed within the frameworks of the available models.

* Corresponding author. Tel.: +86 551 559 5185; fax: +86 551 559 1149.
E-mail address: zhangrr@hmfl.ac.cn (R.R. Zhang).

0925-8388/$ – see front matter © 2011 Elsevier B.V. All rights reserved.
doi:10.1016/j.jallcom.2011.12.119

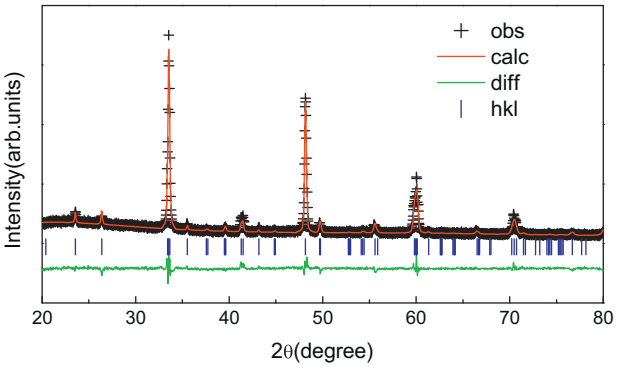

Fig. 1. XRD patterns at room temperature for $Bi_{0.3}Ca_{0.7}Mn_{0.75}Cr_{0.25}O_3$. The observed and calculated patterns are shown as the cross markers and the top solid line, respectively. The vertical markers stand for the angles of calculated Bragg reflections. The lowest solid line represents the difference between the calculated and observed intensities. The fit was done assuming the space group *Pnma*.

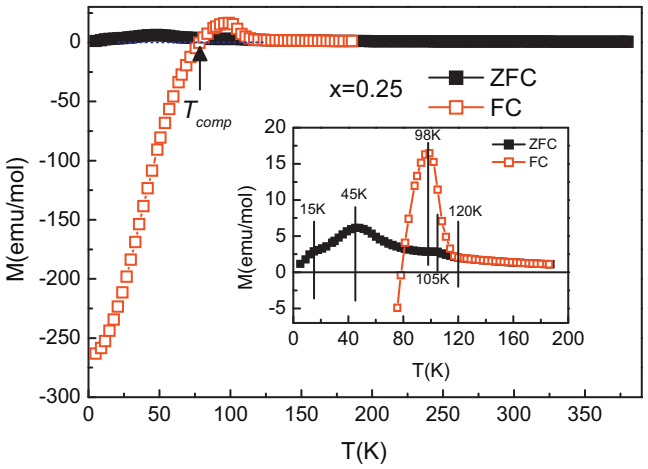

Fig. 2. Temperature dependence of magnetization for $Bi_{0.3}Ca_{0.7}Mn_{0.75}Cr_{0.25}O_3$ under ZFC and FC modes, respectively. The inset is the magnifying of $M(T)$ curves in the part of the temperature range 5–170 K.

2. Experiment

Polycrystalline sample of nominal $Bi_{0.3}Ca_{0.7}Mn_{0.75}Cr_{0.25}O_3$ (BCMCO) composition was prepared by a conventional solid state reaction method. Stoichiometric mixtures of Bi_2O_3, $CaCO_3$, Cr_2O_3 and MnO_2 were ground and pressed into pellets, which were heated in air at 1023 K and 1223 K for 20 h with intermediate grinding. Then the homogenized powders were pressed into cylindrical pellets and subjected to heat treatment for 20 h at 1273 K. After calcinations, the sample was reground, pelletized again, and the final heat treatment was performed for 20 h at 1373 K in air.

Powder X-ray diffraction (XRD) measurement was performed using a Philips X'pert PRO X-ray diffractmeter with Cu K_α radiation and its microstructure was observed by field emission scanning electron microscopy (FE-SEM, FEI Sirion 200 type) at room temperature. The temperature dependence of magnetization was measured using a Quantum Design superconducting quantum interference device (SQUID) MPMS system ($1.8\,K \le T \le 400\,K$, $0\,T \le H \le 5\,T$).

3. Results and discussion

The room temperature XRD pattern of the sample is shown in Fig. 1. The result shows that the sample is single phase with no detectable secondary phases. The XRD patterns of the sample can be indexed by orthorhombic lattice with the space group *Pnma*. The fitting between the experimental spectra and the calculated values using the standard Rietveld technique [16] is rather good, based on the consideration of low R_p value [$R_p = 5.17$ for Fig. 1]. The refined lattice parameters of BCMCO are $a = 5.3577(5)$ Å, $b = 7.5517(1)$ Å and $c = 5.3242(4)$ Å. The cell parameters in the sample, indicating O-type distorted perovskite structure without the cooperative Jahn–Teller (JT) effect due to the separate local distortion each other induced by Cr doped. The resulting Mn—O bond lengths of 1.9237 Å and 1.9310 Å (basal plane) and 1.9250 Å (apical distance) at room temperature are observed. The calculated average bond angle ⟨Mn—O—Mn⟩ is about 157.19°, which deviates from 180° in ideal perovskite structure. The surface morphology and composition of the samples was examined by a SEM accompanied with an energy dispersive spectrometer (EDS). The SEM micrograph shows a granular structure for the sample with a highly dense morphology. The EDS analysis indicates that the cationic ratio is in good agreement with the nominal one within the limit of the experimental error.

Fig. 2 shows the temperature dependence of the magnetization of the BCMCO sample under zero-field-cooling (ZFC) and field-cooling (FC) modes at $H = 100$ Oe. No difference between the ZFC ($M_{zfc}(T)$) and FC ($M_{fc}(T)$) magnetization is observed down to 120 K. However, as $T < 120$ K, both $M_{zfc}(T)$ and $M_{fc}(T)$ curves begin to bifurcate following entirely different paths. For the sake of clarity, the magnified $M(T)$ curve is displayed in the inset of Fig. 2. In the ZFC mode, $M_{zfc}(T)$ curve shows a small shoulder at 105 K. As the temperature decreases, magnetization increases continually until reaching a maximum at 45 K. As temperature decreases further, the $M_{zfc}(T)$ curve shows a kink at about 15 K, implying that there exists a complex magnetic interaction in the BCMCO. Similar phenomenon was also reported by Sun et al., it was attributed to the developing of two distinctive AFM interaction (Mn^{3+}—O—Mn^{3+} and Cr^{3+}—O—Cr^{3+}) with different coupling constants [17]. In a similar manner, we can assign the double-step dropping feature below 45 K to two distinctive FM interaction (Mn^{3+}—O—Mn^{4+} and Mn^{3+}—O—Cr^{3+}). In contrast, the FC magnetization increases below 120 K, goes through a maximum at $T_P = 98$ K, then decreases and passes a zero value of magnetization ($M = 0$) at the compensation temperature ($T_{comp} = 78.5$ K). As $T < T_{comp}$, the magnetization is negative down to the lowest temperatures. This is a typical MR behavior. Moreover, no hysteresis behavior was observed as the FC magnetization was measured in the process of cooling (FCC) and warming (FCW) the sample (not shown here).

The occurrence of MR in perovskite structures is not without precedents. For example, MR phenomenon occurring in $LaVO_3$ is ascribed to the combined effects of Dzyaloshinsky–Moriya (D–M) interaction [18,19] and a magnetostrictive distortion induced by orbital moments [20], whereas the MR occurring in the isostructural YVO_3 is suggested to originate from the competition between single ion anisotropy and D–M interaction [21]. However, for MR appearing in both $NdVO_3$ and $SmVO_3$, it is explained according to N-type ferrimagnetism arising from the imbalance of the quenching rate of the orbital moments of V^{3+} ions [22,23]. For MR occuring in $LnCrO_3$, it is attributed to the polarization of the paramagnetic (PM) moments of the Ln ions which align opposite to the canted Cr moments [24]. Besides of MR observed in the studied BCMCO, this phenomenon was also found previously in different manganites, such as (Dy,Ca)MnO_3 [25], $Gd_{0.67}Ca_{0.33}MnO_3$ [26], $La_{1-x}Gd_xMnO_3$ [27], $NdMnO_{3+\delta}$ [28], $Nd_{1-x}Ca_xMnO_y$ [29], and (Nd,Ca)(Mn,Cr)O_3 [30]. The MR phenomenon in these compounds was interpreted as a manifestation of a ferrimagnetic-like behavior due to the interplay of two magnetic antiferromagnetically coupled sublattices (rare-earth sublattice and Mn sublattice). According to the orbital/energy level structure of Bi ($5d^{10}6s^26p^3$), the outer orbital/energy level of Bi^{3+} has a $5d^{10}6s^2$ structure, in which a $6s^2$ lone pair exists. As a result, Bi^{3+} ion is not a magnetic ion, ruling out the competition between the Bi and Mn/Cr sublattices as the origin of negative magnetization. Moreover, no difference of the FCC and FCW $M(T)$ curves (lower inset of Fig. 3) and no peaks in the specific heat temperature dependence curve indicate that there does not exist any

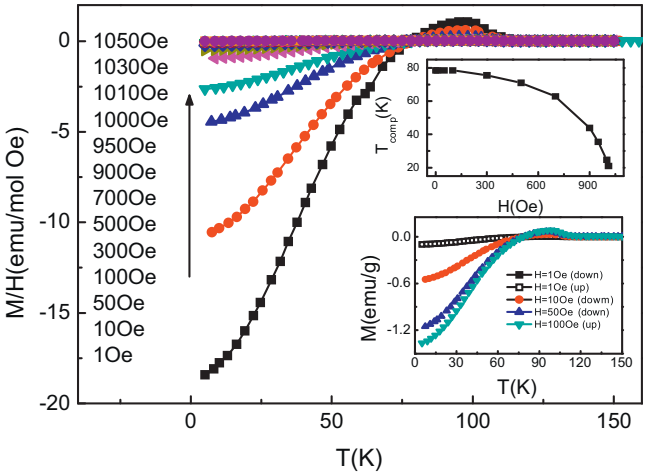

Fig. 3. FC magnetizations normalized to the measuring field as a function of temperature at different fields. The upper inset shows the plot of compensation temperature as a function of measuring field. The lower inset shows the magnetization versus temperature for low applied fields ($H \leq 100$ Oe).

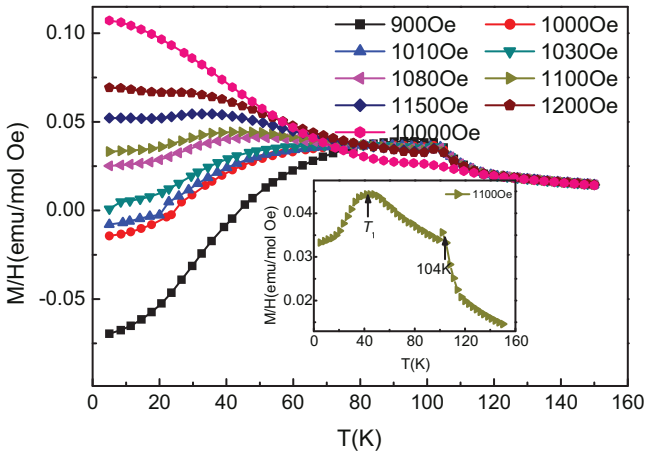

Fig. 4. FC magnetization normalized to the measuring field as a function of temperature at fields $H \geq 900$ Oe. The inset shows the data of FC curves at field $H = 1100$ Oe. The arrow indicates the two characteristic temperatures.

structural phase transition in our sample, excluding the mechanism explaining the origin of MR occurring in $LaVO_3$ as possibility interpreting the origin of MR appearing in our studied sample. What is the mechanism for MR in the BCMCO compound? To make clear this question, we measure the magnetization of BCMCO sample in detail.

Fig. 3 shows the $M_{fc}(T)$ curves (normalized to the measuring field) measured under different applied fields. At low field ($H \leq 100$ Oe), the negative component of the magnetization increases with the increasing of applied magnetic field accompanied by nearly no change of T_{comp}, as shown in the inset of Fig. 3. However, as $H > 100$ Oe, both the negative component of the magnetization and T_{comp} decrease with increasing applied fields. The variation of T_{comp} with the applied field can be reflected as in the inset of Fig. 3. The actual compensation temperature ($T_{comp} = 78.5$ K) is taken as the extrapolated value at $H = 0$. Moreover, between 120 K and T_{comp}, the value of the M/H decreases with the increasing of the applied fields. This observation of non-linear field dependence in the magnetization has also been previously reported by Sudyoadsuk et al. [31], it was explained as a small remanence arising from the presence of a FM clusters. For $H \geq 1030$ Oe, one can observe only positive FC magnetization. In order to clarify the variation of $M(T)$ with applied fields, some $M(T)$ curves under typical fields are plotted in Fig. 4. When $H > 900$ Oe, magnetization shows a plateau in the narrow temperature range of 20 K below 104 K, then decreases with the decreasing of temperature. As $H > 1030$ Oe, the $M(T)$ curves show a peak at around 104 K, which corresponds with the peak at 105 K in the $M_{zfc}(T)$ curve. This result indicates that the transition at 105 K may be of feature of AFM transition. Then the magnetization increases with the decreasing of temperature. Subsequently, with the decreasing of temperature, magnetization starts to decrease at a certain temperature T_1, which shows in the inset of Fig. 4. However, when the field is large enough, for example, $H = 1$ T, the transition temperature T_1 disappears and the magnetization increases with decreasing temperature.

To elucidate the magnetization behavior, isotherm magnetization curves were measured at some typical temperatures between 5 and 300 K. For each measurement, the sample was cooled to the measured temperature from 300 K under the zero field, the results were shown at Fig. 5. It shows that magnetization rises sharply with the increase of the applied field at low fields and does not saturate up to 45 kOe as $T \leq 45$ K. In addition, Fig. 5 displays that the magnetization value of 15 K at high fields is larger than that of other temperatures, which is consistent with the above result that a double-step occurs below 45 K in the $M_{zfc}(T)$ curve. For both $T = 98$ K and 105 K, there is a large H_C can be observed in the inset of Fig. 5, but the magnetization does not saturated up to 45 kOe and shows only a linear variation with H as expected for an antiferromagnet. At high temperature ($T \geq 120$ K), the $M(H)$ plots become linear indicating a typical PM behavior. The $M(H)$ results reveal that the magnetic properties of the sample occur some complex change below 45 K. Even the weak FM moment appears below 120 K, the clear FM hysteresis loop (that is, having square like form) is developed only below 45 K. Additionally, as the temperature increases, the hysteresis loop shrinks and the coercive field H_C decreases. The temperature dependence of H_C is shown in the inset of Fig. 5.

By simple inspection of above results, the complicated magnetic properties of present sample can be unambiguously assigned to the introduction of Cr ions. It is well known that Cr^{3+} ions suppress CO and OO in half doped manganites [32,33] and induce a FM metallic state under zero magnetic field. This fact has been ascribed to the possibility of these cationic species to exhibit itinerant electrons in oxides with valence state that possibly participate in the double exchange [17,32,33]. Conversely a superexchange interaction between Cr^{3+} and Mn^{3+} have been suggested [2,34,35], although some authors suggest a FM spin alignment, whereas others think that Cr^{3+} substitutes Mn^{3+} with opposite spin. Recently,

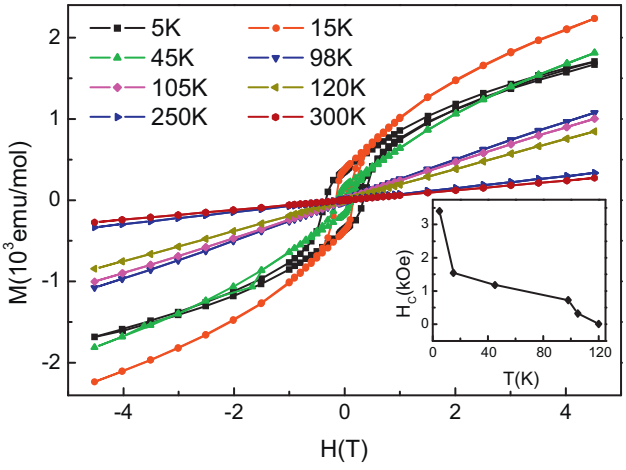

Fig. 5. Magnetization as a function of field at different temperatures in ZFC mode. The inset shows the coercivity as a function of temperature.

Capogna et al. [36] and Martinelli et al. [37] present that only the Mn ions are FM ordered along the z axis, whereas Cr^{3+} ions act as random impurities based on the result of the neutron powder diffraction. For BCMCO sample studied here, the ground state of the parent compound $Bi_{0.3}Ca_{0.7}MnO_3$ is a CO/OO AFM insulator with a Wingner-crystal (WC) mode, in which the real space ordering of Mn^{3+}/Mn^{4+} ions takes place at $T_{CO} \approx 287$ K [14]. Below ~133 K, local spin moments are antiferromagnetically ordered, which consists of FM zigzag chains of Mn^{3+}/Mn^{4+} cations and the $3d^4$ atoms placed as far apart as possible in the (ab) plane, and the coupling between chains is AFM [38]. As the Cr^{3+} substitutes Mn^{3+}, because Cr^{3+} and Mn^{3+} placed as far apart as possible in the plane, the FM interaction between Cr^{3+} and Mn^{3+} is impossible. The suppression of the CO state and the hysteresis loop at low temperature in the system can be understood based on the breaking of the zigzag FM chains and concomitant charge frustration. Considering first the magnetic order, the WC phase consists of zigzag FM chains that are easily cut down by lattice defects, leading to a substantial increase in the kinetic energy. However, the competing FM phase has a two-dimensional character, which is much more robust against lattice defects. For a pure system, the JT coupling favors the long-range staggered CO pattern. In real cases, the B-site substitution should be randomly distributed between the B1 sites (with higher charge density) and B2 sites (with lower charge density) with the same probabilities. This randomness of B-site substitution can break the original CO state, causing charge frustration. This frustration will spread over the whole lattice and lead to the collapse of the long-range CO. Hence, the lattice defects induced by this substitution destabilize the WC phase, which will transform into (1) the FM metallic competing state, (2) a regime with short-range FM clusters, or (3) a spin-glass state, depending on couplings and on the B-site substitution [39]. Thus we assume the Cr ions acting as random impurities in our system.

As discussed above, the possibility for negative magnetization may be supposed by the polarization of the PM moments in a direction opposite to the direction of the applied magnetic field, as observed in some $LnCrO_3$ [24,40,41] and Sr_2YbRuO_6 [42]. This PM moment, arising from the unordered Cr moments, can polarize against the canted field of Mn moments as in the case of $LnCrO_3$ compounds. If we consider this polarization as the cause of MR, then the measured magnetization M should follow equation [24]

$$M = M_{Mn} + \frac{C_{Cr}(H_I + H_a)}{T - \theta} \quad (1)$$

where M_{Mn} is the canted moment of Mn, H_I is the internal field due to the canted Mn moment, H_a is the applied field, C_{Cr} is the Curie constant and θ is the Weiss constant. The limitation of this analysis is the assumption that M_{Mn} and H_I are independent of temperature, which is usually true if $T \ll T_N$. In the present case, this may not be true and hence the value obtained will only be an approximation. The solid line in Fig. 6 shows the fit to the $M(T)$ curve ($H = 100$ Oe) using the above equation. The parameters obtained from the fit are $M_{Mn} = 299 \pm 34$ emu/mol, $H_I = -10061 \pm 1797$ Oe and $\theta = -50$ K. These values are comparable to those obtained for $GdCrO_3$ [40] and Sr_2YbRuO_6 [42]. The value of C_{Cr} (=3.87) used in the analysis was obtained from the free ion Cr^{3+} PM susceptibility above T_N. The good fitting to the equation in Fig. 6 indicates the presence of a considerable fraction of Cr moments that are PM and contribute to the polarization against the canted Mn moments. The positive value of M_{Mn} is consistent with the result that the FC magnetization goes through a positive maximum before reaching the compensation point. The negative value of the internal field H_I highlights its direction against both the applied field and the canted Mn moments. Moreover, the $M(T)$ curve shows a strong deviation from the fitting curve at low temperature. That is, the Cr moments start ordering at 98 K due to the large internal field from the ordered

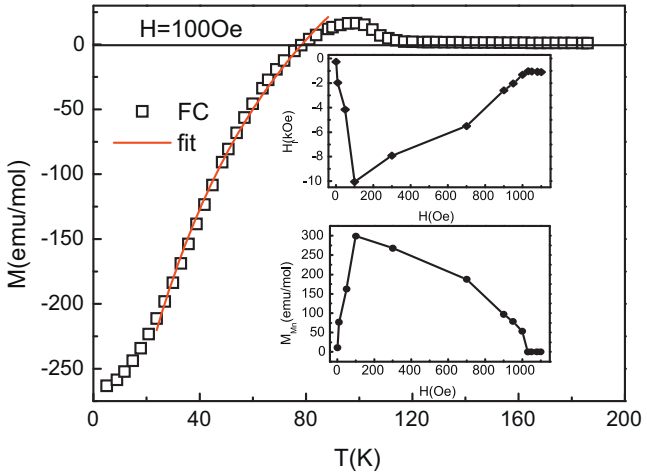

Fig. 6. FC magnetization of BCMCO for 100 Oe. The solid line is the fit to Eq. (1) in the text. Variation of the canted Mn moment (M_{Mn}) and the internal field (H_I) due to ordered Mn moments obtained from the fit for different applied fields are given as insets.

Mn moments, but complete the ordering at 20 K. For other applied field values, the good fitting of $M(T)$ to Eq. (1) is also found (not shown here). The inset of Fig. 6 shows the variation of M_{Mn} (lower) and H_I (upper) at $H < 1050$ Oe. The variation of these components is in good agreement with the observed magnetization behavior. The absolute value of internal field shows an initial increase with the applied field, but decreases at higher fields. The initial increase is consistent with the increase in negative magnetization for low magnetic field (shown in the inset of Fig. 3). The good fitting is consistent with our previous hypothesis, which proves that only the Mn ions have canting spin structure, whereas Cr^{3+} ions act as random impurities in our compound.

The consistency between the theory and the experimental data should be attributed to two important aspects. First, the coercivity is very large at low temperature. For example, at 45 K where the FC magnetization decreases drastically, the coercivity H_C with 0.118 T is much larger than the applied field (0.01 T). In this case, it is impossible that the magnetic domains which are antiparallel with the applied field flip to the H direction under the action of the applied field. Secondly, we believe that M_{Mn} is parallel to the H direction while M_{Cr} is antiparallel to it. Thus the fitting will be adaptable. When the system is cooled down to 120 K in the process of FC, which is below the magnetic ordering temperature, the sample exists FM cluster induced by Cr-doping. As the temperature decreases, the disordered Cr^{3+} ions become to polarize against the canted field of Mn moments. As a result, the net magnetization of the system is $M_s = M_{Mn} - M_{Cr}$. Keeping these two aspects in mind, we can understand the $M_{fc}(T)$ curves clearly. As the temperature decreases from 98 K, M_{Cr} increases much faster than M_{Mn}. The 78 K corresponding to $M_s = 0$ is the compensation point of the magnetization of the two sublattices. As $T > 78$ K, M_{Mn} is larger than M_{Cr} because M_{Cr} is induced by M_{Mn}, which results in the net magnetization $M_s > 0$ in the temperature range from 98 K to 78 K (see Fig. 2). Below 78 K, M_{Cr} is much larger than M_{Mn}. Since the coercivity of the system is much larger than the applied measuring field (as shown in the inset of Fig. 5), the magnetic domains are locked in the original direction and M_{Cr} remains antiparallel to the applied field. Therefore the net magnetization should be a negative value. At low temperature, the fitted curve deviates from the experimental data because of the magnetic ordering of Cr moments. Taking into account this situation, the variation of $M_{fc}(T)$ curves under higher applied field can be explained reasonably. For example, in the process of ZFC process, the magnetic ions are locked in random directions during cooling

in zero field. When a measuring field of 0.01 T is applied at 5 K, the magnetic ions are aligned along the applied field. Therefore, the $M_{zfc}(T)$ curve exhibits a kink 15 K and a peak at 45 K instead of the MR phenomenon in the $M_{fc}(T)$ curve at low temperature.

4. Conclusions

In summary, the MR phenomenon below the magnetic ordering temperature is observed in BCMCO sample in the process of FC magnetization measurement as the applied field is below 1030 Oe. Meanwhile, both compensation temperature and negative magnetization are also found in $M_{fc}(T)$ curve. The analysis of magnetization measurement results clearly indicates the presence of two components in the magnetic ordering, which is suggested to come from the contribution of Mn^{3+}/Mn^{4+} and Cr^{3+}moments. The MR phenomenon observed in BCMCO sample is suggested to stem from the antiparallel coupling of the Cr^{3+} moments and the canted $Mn^{3+/4+}$ moments. However, in order to provide an exact explanation for the observed anomalous behavior, detailed neutron diffraction and field-cooled X-ray magnetic circular dichroism measurements will be necessary.

Acknowledgments

This work was supported by the National Key Basic Research under contract no. 2007CB925002, and the National Nature Science Foundation of China under contract nos. 10774146, 10804111, 50672099, 11104275 and Director's Fund of Hefei Institutes of Physical Science, Chinese Academy of Sciences.

References

[1] T. Kimura, Y. Tomioka, R. Kumai, Y. Okimoto, Y. Tokura, Phys. Rev. Lett. 83 (1999) 3940.
[2] R. Mahendiran, M. Hervieu, A. Maignan, C. Martin, B. Raveau, Solid State Commun. 114 (2000) 429–433.
[3] V. Hardy, A. Maignan, S. Héber, C. Martin, Phys. Rev. B 67 (2003) 024401.
[4] C. Yaicle, C. Frontera, J.L. García-Muñoz, C. Martin, A. Maignan, G. André, F. Bourée, C. Ritter, I. Margiolaki, Phys. Rev. B 74 (2006) 144406.
[5] T. Kimura, R. Kumai, Y. Okimoto, Y. Tomioka, Y. Tokura, Phys. Rev. B 62 (2000) 15021.
[6] Joonghoe Dho, W.S. Kim, N.H. Hur, Phys. Rev. Lett. 89 (2002) 027202.
[7] R. Tasaki, S. Fukushima, M. Akaki, D. Akahoshi, H. Kuwahara, J. Appl. Phys. 105 (2009) 07D725.
[8] H. Woo, T.A. Tyson, M. Croft, S.W. Cheong, J.C. Woicik, Phys. Rev. B 63 (2001) 134412.
[9] N.A. Hill, K.M. Rabe, Phys. Rev. B 59 (1999) 8759.
[10] A. Kirste, M. Goiran, Phys. Rev. B 67 (2003) 134413.
[11] C.M. Xiong, J.R. Sun, R.W. Li, S.Y. Zhang, T.Y. Zhao, B.G. Shen, Appl. Phys. Lett. 95 (2004) 1336.
[12] D. Tzankov, D. Kovacheva, K. Krezhov, R. Puźniak, A. Wiśniewski, E. Svàb, M. Mikhov, J. Phys.: Condens. Matter. 17 (2005) 4319.
[13] O. Toulemonde, I. Skovsen, F. Mesguich, E. Gaudin, Solid State Sci. 10 (2008) 476–480.
[14] R.R. Zhang, G.L. Kuang, X. Luo, Y.P. Sun, J. Alloys Compd. 484 (2009) 36–39.
[15] L. Luan, Z. Qu, S. Tan, X. Xin, Y.H. Zhang, J. Magn. Magn. Meter. 312 (2007) 107–116.
[16] D.B. Wiles, R.A. Young, J. Appl. Cryst. 14 (1981) 149–151.
[17] Y. Sun, W. Tong, X. Xu, Y.H. Zhang, Phys. Rev. B 63 (2001) 174438.
[18] I. Dzyaloshinsky, J. Phys. Chem. Solids 4 (1958) 241–255.
[19] T. Moriya, Phys. Rev. 120 (1960) 91–98.
[20] H.C. Ngueyen, J.B. Gooodenough, Phys. Rev. B 52 (1995) 324.
[21] Y. Ren, T.T.M. Palstra, D.I. Khomskii, E. Pellegrin, A.A. Nugroho, A.A. Menovsky, G.A. Sawatzky, Nature 396 (1998) 441–444.
[22] Y. Kimishima, Y. Chiyanagi, K. Shimizu, T. Mizuno, J. Magn. Magn. Mater. 210 (2000) 244–250.
[23] Y. Kimishima, M. Uehara, T. Saitoh, Solid State Commun. 133 (2002) 559–564.
[24] A.H. Cooke, D.M. Martin, M.R. Wells, J. Phys. C: Solid State Phys. 7 (1974) 31333.
[25] C.A. Nordman, V.S. Achutharaman, V.A. Vas'ko, P.A. Kraus, A.R. Ruosi, A.M. Kadin, A.M. Goldman, Phys. Rev. B 54 (1996) 9023.
[26] G.J. Snyder, C.H. Booth, F. Bridges, R. Hiskes, S. DiCarolis, M.R. Beasley, T.H. Geballe, Phys. Rev. B 55 (1997) 6453.
[27] J. Hemberger, S. Lobina, H.A. Krug Von Nidda, N. Tristan, V. Yu Ivanov, A.A. Mukhin, A.M. Balbashov, A. Loidl, Phys. Rev. B 70 (2004) 024414.
[28] F. Bartolomé, J. Herrero-Albillos, L.M. Garcia, J. Bartolomé, N. Jaouen, A. Rogalev, J. Appl. Phys. 97 (2005) 10A503.
[29] I.O. Troyanchuk, V.A. Khomchenko, G.M. Chobot, A.I. Kurbakov, A.N. Vasil'ev, V.V. Eremenko, V.A. Sirenko, M. Yu Shveum, H. Szymczak, R. Szymczak, J. Phys.: Condens. Matter. 15 (2003) 8865–8880.
[30] I.O. Troyanchuk, M.V. Bushinsky, V.V. Eremenko, V.A. Sirenko, H. Szymczak, Low Temp. Phys. 28 (2002) 45.
[31] T. Sudyoadsuk, R. Suryanaryanan, P. Winotai, L.E. Wenger, J. Magn. Magn. Mater. 278 (2004) 96–106.
[32] A. Maignan, F. Damay, C. Martin, B. Raveau, Mater. Res. Bull. 32 (1997) 965–972.
[33] C. Martin, A. Maignan, F. Damay, M. Hervieu, B. Raveau, Z. Jirak, G. André, F. Bourée, J. Magn. Magn. Mater. 202 (1999) 11–21.
[34] O. Cabeza, M. Long, C. Severac, M.A. Bari, C.M. Muirhead, G.M. Francesconi, C. Greaves, J. Phys.: Condens. Matter. 11 (1999) 2569–2578.
[35] R. Gundakaram, A. Arulraj, P.V. Vanitha, C.N.R. Rao, N. Gayathri, A.K. Raychaudhuri, A.K. Cheetham, J. Solid State Chem. 127 (1996) 354–358.
[36] L. Capogna, A. Martinelli, M.G. Francesconi, P.G. Radaelli, J. Rodriguez Carvajal, O. Cabeza, M. Ferretti, C. Castellano, T. Corridoni, N. Pompeo, Phys. Rev. B 77 (2008) 104438.
[37] A. Martinelli, M. Ferretti, C. Castellano, M.R. Cimberle, C. Ritter, J. Phys.: Condens. Matter. 20 (2008) 145210.
[38] S. Grenier, V. Kiryukhin, S.W. Cheong, B.G. Kim, J.P. Hill, K.J. Thomas, J.M. Tonnerre, Y. Joly, U. Staub, V. Scagnoli, Phys. Rev. B 75 (2007) 085101.
[39] X. Chen, S. Dong, K.F. Wang, J.M. Liu, E. Dagotto, Phys. Rev. B 79 (2009) 024410.
[40] K. Yoshii, J. Solid State Chem. 159 (2001) 204–208.
[41] K. Yoshii, A. Nakamura, Y. Ishii, Y. Morii, J. Solid State Chem. 162 (2001) 84–89.
[42] Ravi P. Singh, C.V. Tomy, J. Phys.: Condens. Matter. 20 (2008) 235209.